Millimeter-Wave CMOS Impulse Radio

Ahmet Oncu[1,2] and Minoru Fujishima[1]
[1]*Hiroshima University*
[2]*The University of Tokyo*
Japan

1. Introduction

Millimeter waves are electromagnetic waves with wavelengths of 1 to 10 mm in vacuum, and they were discovered experimentally in the 19th century (Wiltse, 1984). In 1946, the most unique feature of millimeter waves, oxygen absorption at 60 GHz, was reported, which results in the rapid attenuation of electromagnetic waves in the air (Beringer, 1946). Although the oxygen absorption makes long-distance wireless communication difficult, it enables us to allocate a wide frequency band, which realizes ultra-high-speed communication greater than 1Gbps (gigabits-per-second). Recently, the well-known feature of millimeter-wave communication has attracted attention again because millimeter-wave circuits have been realized with advanced CMOS technologies, and the recent 60GHz band license-free regulations with license-free bandwidths of 9GHz in Europe and 7GHz in Japan, USA, Canada and Korea. In academic conferences and journals, many studies on millimeter-wave CMOS circuits were reported in the past few years, and consumer devices are expected to be available soon.
Here, for realizing the consumer application of millimeter waves, the reduction of power consumption is the most important issue. It is noted that the power-hungry building blocks in a transceiver are the local oscillator (LO) based on the phase-locked loop (PLL), and analog-to-digital and digital-to-analog converters (ADC and DAC) as shown in Fig. 1(a) (Marcu, 2009). If these blocks can be eliminated partially or completely in a transceiver, power consumption will be considerably reduced. From this viewpoint, we have studied millimeter-wave pulse communication for high-performance CMOS wireless transceivers as shown in Fig. 1(b) and Fig. 1(c). In this study, low-power direct pulse generators, high-speed switches and receivers, which are the most important building blocks in millimeter-wave pulse communication, are discussed for high-speed wireless communications using the 60 GHz band. In conclusion, the prospects for millimeter-wave pulse communication will be addressed.

2. 60GHz CMOS pulse transmitter

In this section, three low-power 60GHz CMOS pulse transmitter circuits are presented. The first one is a carrier-less direct pulse generator circuit, (Badalawa, 2007). The second design presents an 8Gbps millimeter-wave CMOS switch used for an Amplitude Shift Keying (ASK) modulator (Oncu, 2008, b) and the last one presents a design of a low-power 10Gbps

Source: Advances in Solid State Circuits Technologies, Book edited by: Paul K. Chu,
ISBN 978-953-307-086-5, pp. 446, April 2010, INTECH, Croatia, downloaded from SCIYO.COM

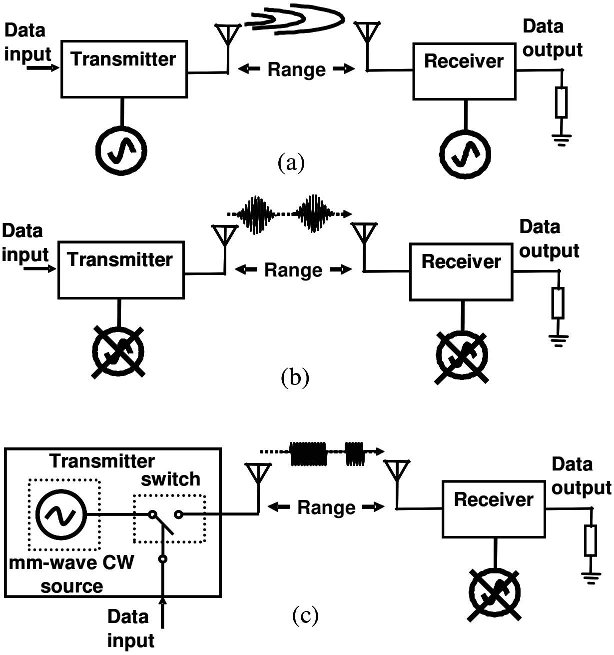

Fig. 1. Block diagram of wireless communication based on (a) carrier modulation, (b) direct pulse generator without oscillator, (c) pulse generator with millimeter-wave oscillator.

CMOS transmitter for a 60GHz millimeter-wave impulse radio, where a 60GHz millimeter-wave continues-wave (CW) source and ASK modulator circuits are embedded on the same silicon substrate.

2.1 60GHz CMOS pulse generator design

The circuit topology of the proposed pulse generator (PG) is shown in Fig. 2. This circuit has a monopulse generator (MPG) cell is composed of two CMOS inverters to contribute the delay and two NMOS transistors to produce the pulses by combing edges as shown in Fig. 3(a). The inverter A is driven by falling edges of baseband data. Just before the falling edge, NMOSFET C is "off" and NMOSFET D is "on". When the signal passes through inverter A, NMOSFET C is turned "on" and the output node is discharged. Next, when the input signal passes through inverter B, NMOSFET C is turned "off" and the output node is charged by a pulling-up inductor. At this moment, one pulse is produced according to the propagation delay of inverter B. The transmitter can be implemented with a low power consumption using this topology, because the circuit is activated only when falling edges of the input signal are fed from the baseband data. Since no power is consumed at other times, consumed power has a linear relationship with the input data rate.
To fit the delay time per inverter to 8ps, which is being equal to half the reciprocal of the carrier frequency, it is essential to reduce the load capacitance of the transistors that are connected to each inverter output node. To obtain a short delay time, the gate widths of NMOS and PMOS transistors in the inverter should be increased to obtain a large drain

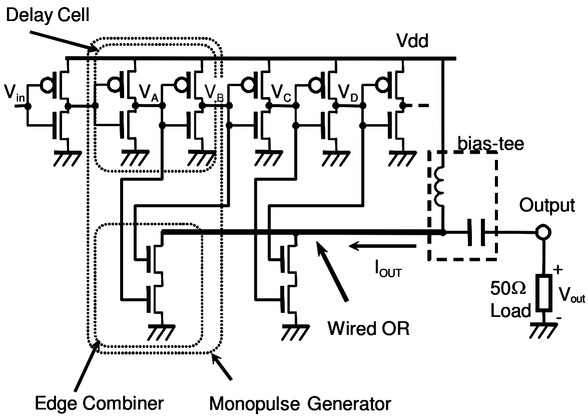

Fig. 2. Circuit topology of a 60GHz CMOS pulse generator.

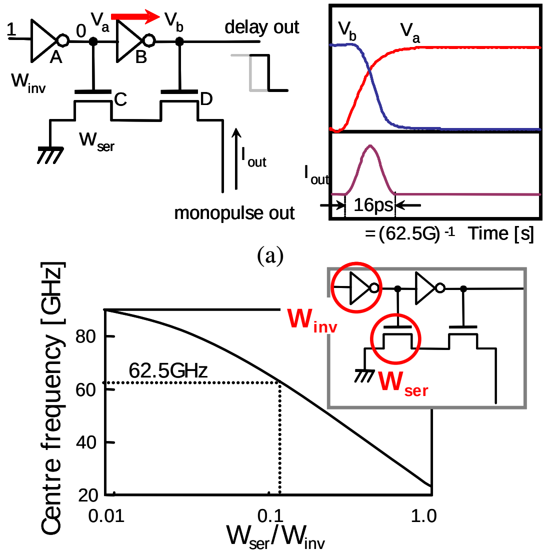

(b)

Fig. 3. (a) An edge combiner comprising MOSFETs C and D has to generate a 16ps pulse. (b) Centre frequency as a function of NMOS width Wser over inverter width Winv.

current. Since the load capacitance connected to the inverter output node is varied favorably or unfavorably with the inverter delay, the relationship between the size of the inverter and the edge combiner NMOSFET is essential to obtain a carrier frequency of 62.5GHz. Figure 3(b) shows the relationship between centre frequency when the fan-out is varied from 0.01 to 1. To realize a 60GHz PG using this circuit topology, the fan-out should be set to 0.1. Not only the optimization, but also selecting of CMOS process with small threshold voltage is one of the key points to implement 60GHz pulse generator as mentioned above. Here, we choose the 9metal TSMC CMOS 90nm process, which has the 1/2 times of small threshold

voltage of the CMOS process used in 22-29GHz UWB CMOS pulse generator circuit in (Fujishima, 2006).
The power spectrum must fit into a spectrum mask to meet regulations as shown in Fig. 4. Here, filtering is employed (Maruhashi, 2005) to satisfy the regulations while increasing the power consumption. To solve these problems, an all-digital low-power CMOS pulse generator with 14 delay stages, which generates a pulse width of 224ps, is adopted. To satisfy the power spectrum regulations without any filters, monopulse amplitudes within a single pulse are adjusted to four levels to approximate the ideal Gaussian power spectrum by sizing the edge-combiner NMOSFET as shown in Fig. 5.

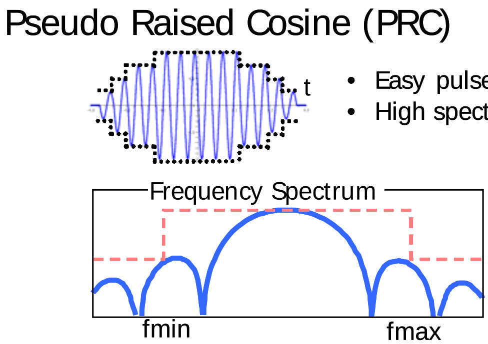

Fig. 4. Pseudo-raised cosine pulse for satisfying specified.

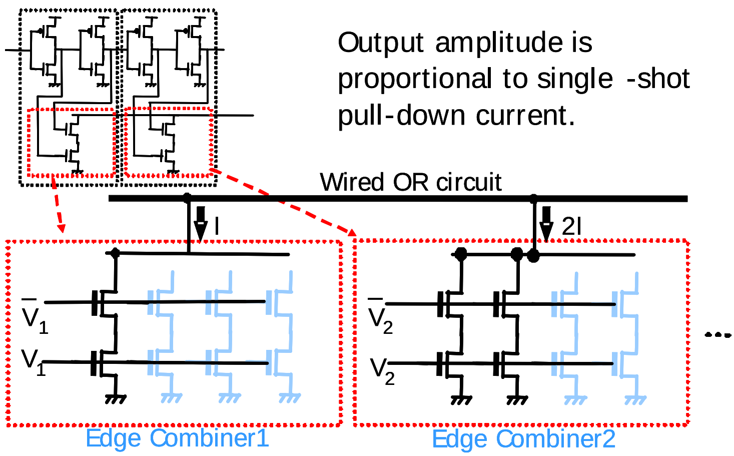

Fig. 5. MOSFET sizing for generating pseudo-raised cosine pulse.

Figure 6 shows a chip micrograph of the CMOS pulse generator with a die area of 590×380μm², where a 90nm CMOS process with nine metal layers was used. The time-domain response of the pulse generator is shown in Fig. 7, where the 62.5GHz operating frequency is observed at a supply voltage of 1.15V, and the four-level approximation is confirmed.

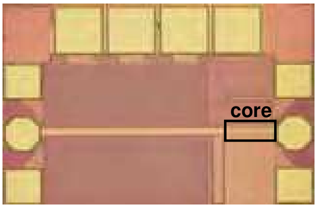

Chip micrograph CMOS 90nm (nine metals one ploy)

Technology	90nm CMOS
Frequency Band	59-66GHz
Modulation	PPK
Supply Voltage	1.15V
Input Data Rate	1.5Gbps
Power Consumption	11mW@ 1.5Gbps
Core Size	90µm×20µm

Fig. 6. Chip micrograph and specification of 60GHz CMOS pulse generator.

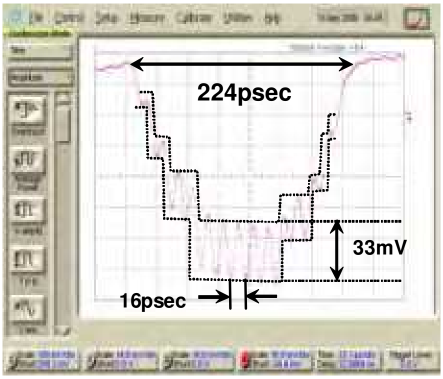

Fig. 7. Measured transient response of 60GHz CMOS pulse generator.

Figure 8 shows carrier frequencies and output powers as function of supply voltage, and also shows power consumptions as function of input data rate. The carrier frequency increased with supply voltage with inverse proportional relationship, while output power is almost unchanged when supply voltage is higher than 0.7V. The linear dependence of power consumption on input data rate is confirmed by the measurement data. Since power is only consumed at rising edges of the input signal, a low average power consumption is observed at 1.5Gbps compared with those in (Maruhashi, 2005; Nakakita, 1997). The power consumption for the proposed pulse generator is 11.5mW at a supplies voltage of 1.15V.

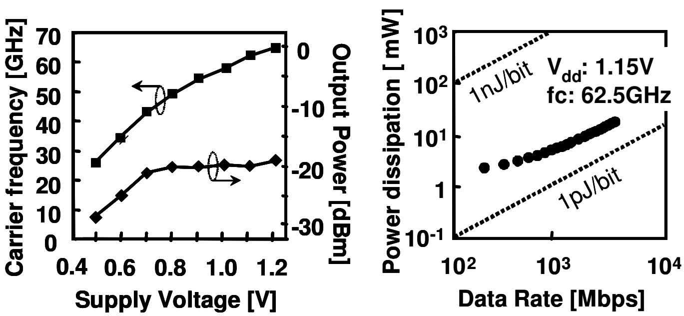

Fig. 8. (a) Carrier frequency and output power as a function of supply voltage and (b) power dissipation as a function of input data rate.

In this section millimeter-wave pulse generator was studied. By designing pulse generators in digital circuits, a 60GHz millimeter-wave pulse can be generated without using a power-hungry LO. As a result, the pulse generator consumes a small amount of power proportional to input data rate. However, this architecture strictly depends on the used technology to achieve higher RF power. We concluded that shorter channel advanced CMOS processes would provide better speed and RF power performance. In the following sections, we study the pulse generator architectures consisting of a low-power millimeter-wave ASK modulator and a 60GHz oscillator in standard CMOS process which is generally used for digital processor design.

2.2 8Gbps 60GHz CMOS ASK modulator

A millimeter-wave CMOS impulse radio with ASK modulator, as shown in Fig. 9, is promising for low-cost and low-power wireless communication, in which a digital switch controls a millimeter-wave CMOS ASK modulator in the transmitter. This architecture will have less sensitivity to the used CMOS technology than that of a direct millimeter-wave pulse generator. The receiver receives 60GHz pulses and converts them to a digital signal (Oncu, 2008, a; Lee, 2009). In this section, we study a design of an 8Gbps CMOS ASK modulator for a 60GHz millimeter-wave impulse radio.

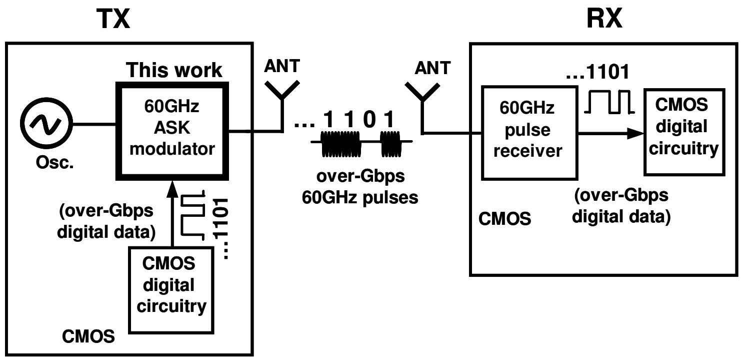

Fig. 9. Block Diagram of millimeter-wave impulse radio with a 60GHz ASK (Amplitude Shift Keying) modulator.

Figure 10(a) shows a conventional millimeter-wave ASK modulator in CMOS (Chang, 2007). It consists of an oscillator and a buffer. Millimeter-wave pulses are obtained by turning the biasing on and off. Although this architecture has high isolation when the biasing is turned off, the switching speed is limited by the stored energy in the oscillator tank. High-speed conventional distributed traveling-wave millimeter-wave ASK modulators in compound semiconductors have been reported (Mizutani, 2000; Ohata, 2000; Ohata, 2005; Kosugi, 2003; Kosugi, 2004). They were realized using distributed shunt switches between the signal and the ground line of a transmission line as shown in Fig. 10(b). In this architecture, when the switches are off the input signal is transferred to the output and the ASK modulator is in the ON state. On the other hand, when the switches are turned on, no input signal is transferred to the output and the ASK modulator is in OFF state. The distributed structure requires a large number of switches since the resistances of the switches in the OFF state should be small to realize a lossy transmission line.

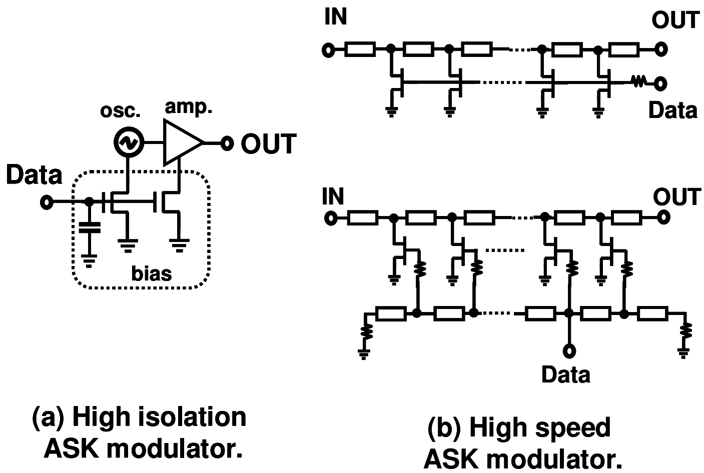

Fig. 10. Architectures of conventional (a) high-isolation and (b) high-speed ASK modulators.

2.2.1 Millimeter-wave CMOS ASK modulator design

A possible distributed CMOS modulator is shown in Fig. 11(a). However, low-quality parasitic capacitances in the switches, which are located on a silicon substrate, are expected to degrade the transmission line characteristics. In this study, a reduced-switch architecture is used for a high-speed millimeter-wave CMOS ASK modulator as shown in Fig. 11(b). Note that the isolation characteristics become degraded upon reducing the number of switches since each switch has a leakage to the output. To achieve high isolation with a reduced number of switches, the transmission line length between switches is adjusted. When the millimeter-wave signal travels from the source to the load, the switches do not only dissipate the incident signal, but they also reflect and leak it as shown in Fig. 12. Note

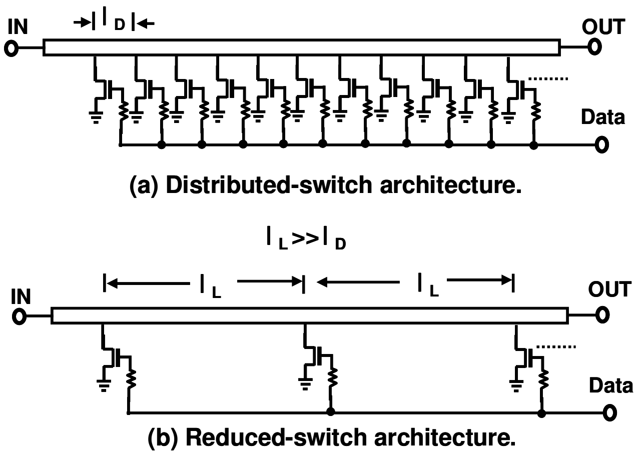

Fig. 11. Architectures of (a) distributive and (b) reduced-switch ASK modulators in CMOS process.

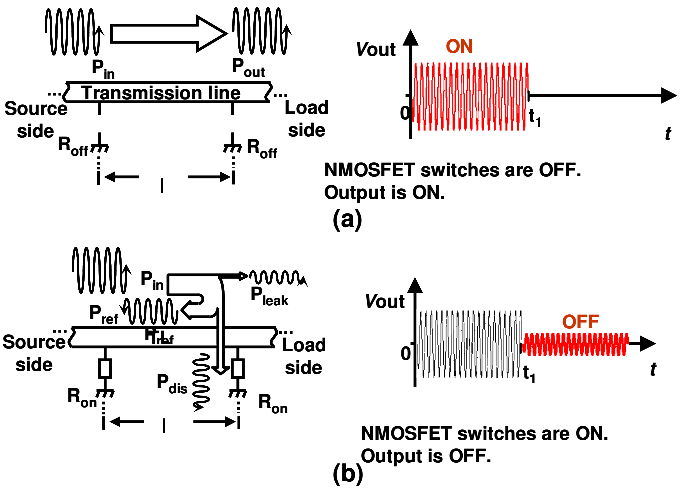

Fig. 12. Illustration of transmitted, reflected, dissipated and leaked signals of a switch in the (a) ON and (b) OFF states of the modulator when the millimeter-wave signal travels from source to the load.

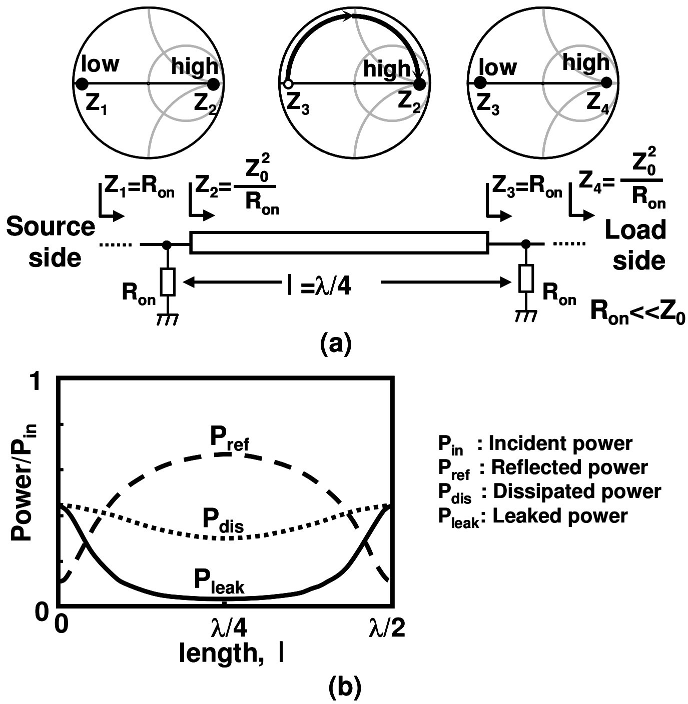

Fig. 13. (a) Impedance transformation along the modulator and (b) calculated reflected, dissipated and leaked powers as a function of the transmission line distance between switches.

that, in a transmission line, impedance transformation between the two terminals occurs as shown in Fig. 13(a). In Fig. 13(b), the calculated leaked, reflected and dissipated powers are shown as a function of the distance between switches. Since the dissipated power in the switches is insensitive to the transmission line length, reflection should be maximized to minimize the leakage. To obtain maximum reflected power and minimum leaked power, the switches are separated by a quarter-wavelength distance. In this case, the isolation is maximized with a lower number of switches.

A 60GHz CMOS ASK modulator is designed with three NMOSFET switches and two quarter-wavelength transmission lines as shown in Fig. 14. When the digital input is 0V, the NMOSFET switches are turned off. Since the parasitic capacitance of each switch in the OFF state is negligible, the input impedance of each transmission line is equal to the load impedance and the input power is transferred to the output. When the digital input is 1V, the switches are turned on. The transmission line with a quarter wavelength transforms the low impedance of the switch to a high impedance and reflection is maximized. In this case, the leaked power to the output is minimized and high isolation is achieved.

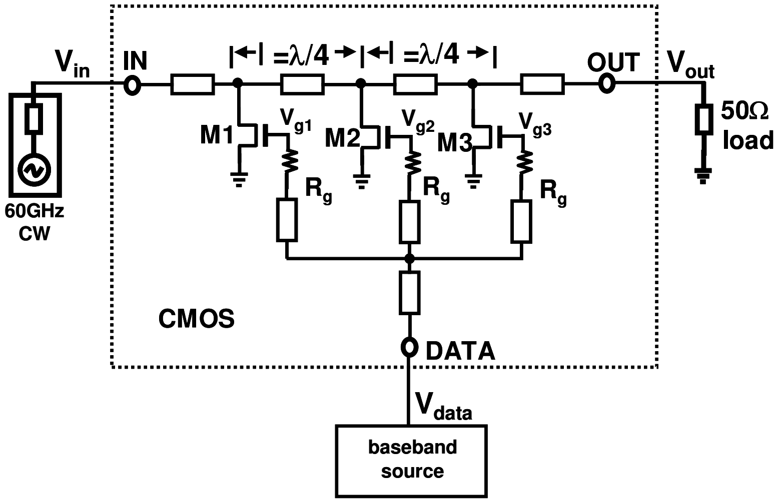

Fig. 14. Circuit schematic of the CMOS ASK modulator for 60GHz wireless communication.

Millimeter-wave NMOSFET models are established by extracting the parasitic components based on on-wafer measurements (Doan, 2005). The slow-wave transmission line (SWTL) (Cheung, 2003) shown in Fig. 15 is used for implementing the quarter-wavelength transmission lines and the networks between the circuit and the pads to reduce the size of the modulator. In the SWTL, a slotted ground shield under the signal line is laid orthogonal to the direction of the signal current flow. This structure results in the propagating waves having lower phase velocity; thus, the corresponding wavelength at a given frequency is reduced. A quarter wavelength is obtained using a 450-μm-long SWTL. Note that the quarter wavelength would be 850μm if a microstrip line (MSL) was used.

200Ω gate resistors are inserted to ensure operation with sufficient high-speed. Transient internal waveforms are simulated as shown in Fig. 16. A 200ps pulse is applied from the data port to analyze the response of the circuit. The total time of the rising and falling gate

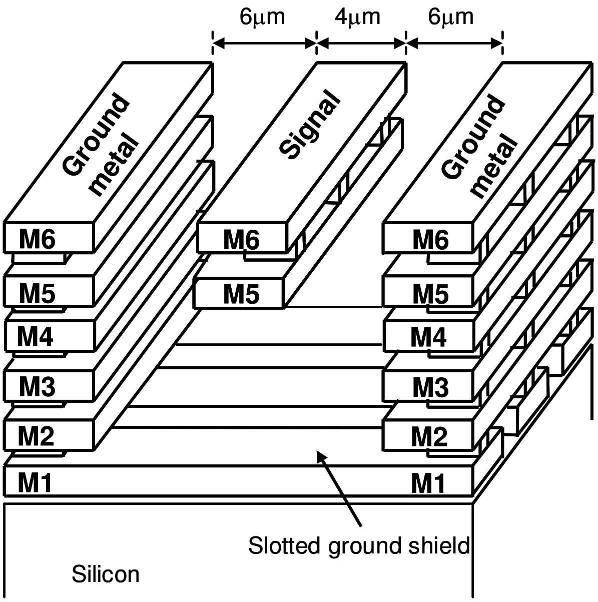

Fig. 15. Structure of the slow-wave transmission line used in the circuit.

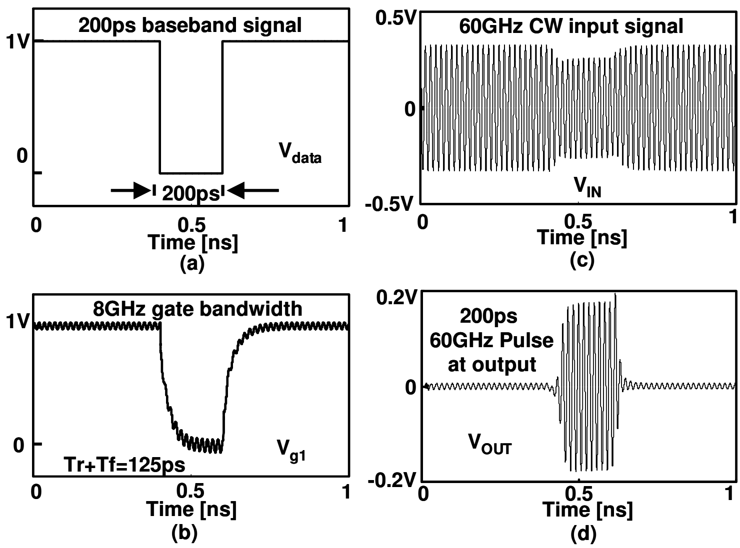

Fig. 16. Transient simulation; (a) 200ps applied data pulse, and responses of (b) the gate voltage of the NMOSFET switch, and (c) input and (d) output signals.

voltages is estimated as 125ps, which corresponds to the maximum data rate of 8Gbps. The 60GHz millimeter-wave ASK modulator is fabricated by a 6-metal 1-poly 90nm CMOS process. The cutoff frequency f_T and the maximum operation frequency of the nMOSFET are 130GHz and 150GHz, respectively. Figure 17 shows a micrograph of the fabricated ASK modulator. The size of the chip is 0.8mm × 0.48mm including the pads. The core size is 0.61mm × 0.3mm.

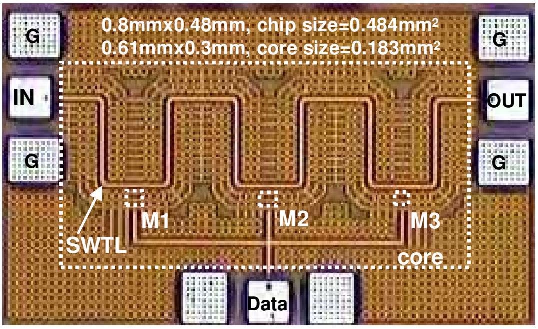

Fig. 17. Micrograph of the fabricated chip.

2.2.2 Experimental result and discussion

On-wafer two-port measurements were performed up to 110-GHz with Anritsu ME7808 network analyzer with transmission reflection modules for the ON and OFF states by applying 0V and 1V DC voltages to the gate terminal, respectively. The measured and simulated insertion losses of the modulator for the two states are shown in Fig. 18(a) for comparison. The insertion losses in the ON and OFF states are 6.6dB and 33.2dB, respectively, at 60GHz. Isolation is defined as the insertion loss difference between the ON and OFF states, which is 26.6dB. The isolation is nearly flat from 20 to 80GHz, although the maximum isolation is measured at 60GHz. As a result, shorter transmission lines may be adopted to reduce the insertion loss caused by the SWTL in the ON state of the modulator. The simulated isolation is shown at frequencies up to 350GHz in Fig. 18(b) to demonstrate

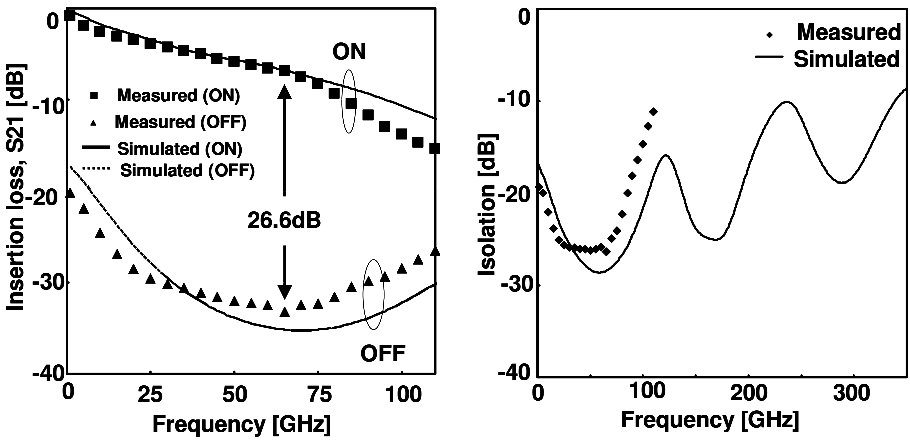

Fig. 18. Measured and simulated (a) insertion loss (S21) of the ASK modulator for ON and OFF states and (b) isolation of the ASK.

the frequency behaviour of the modulator. The minimum isolation appears at 60GHz when the electrical length of the transmission lines is λ/4, where λ is the wavelength. Local maxima in the OFF-state insertion loss occur at 180GHz and 300GHz, which correspond to 3λ/4 and 5λ/4, respectively.

The time-domain response is measured using a 70GHz sampling oscilloscope, a 60GHz millimeter-wave source module and a pattern generator. No external filters are applied in the measurement. A 60GHz continuous wave is applied to the RF input and the modulator is controlled by the pattern generator. The rising and falling times of the applied baseband signal are 6ps and 8ps, respectively. The output response for the maximum data rate is shown in Fig. 19(a). In Fig. 19(b), the output response is shown for a 125ps single-baseband pulse by reducing the scale to 20ps.

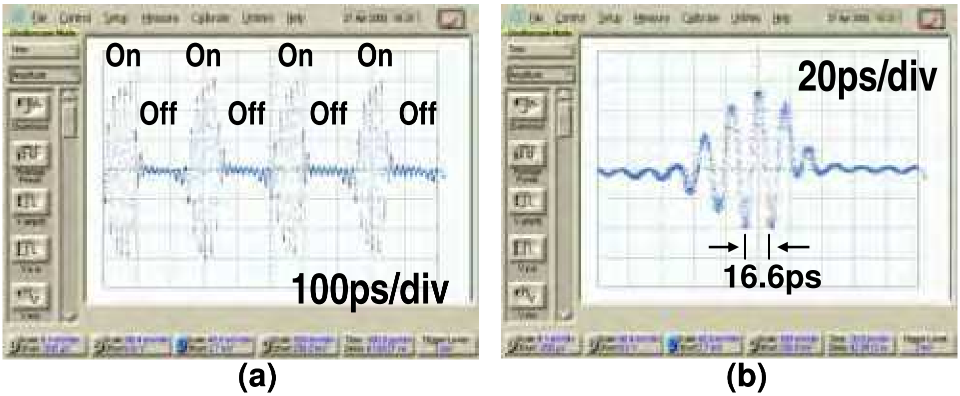

Fig. 19. Measured output response of the modulator for (a) an 8Gbps data train and (b) a single 125ps data pulse.

The maximum data rates as a function of the isolation of the millimeter-wave ASK modulators are shown in Fig. 20. It can be seen that the isolation and the maximum data rate have a tradeoff relationship. The product of the maximum data rate and the isolation of this modulator is 170GHz, which is the highest value among multi-Gbps ASK modulators.

2.3 12.1mW 10Gbps pulse transmitter for 60GHz wireless communication

In this section, we present a design of a low-power 10Gbps CMOS transmitter (TX) for a 60GHz millimeter-wave impulse radio, where a 60GHz millimeter-wave CW source and ASK modulator circuits are embedded on the same silicon substrate as shown in Fig. 21. An 8Gb/s CMOS ASK modulator for 60GHz wireless communication is studied in Section 2.2. This single-pole-single-throw (SPST) reduced NMOSFET switch architecture is capable of high-speed operation without DC power dissipation. Its isolation was maximized by a quarter-wave length transmission line which results in a long transmission lines, therefore the insertion loss becomes high. Figure 22(a) shows TX configuration which consists of an off-chip 60GHz millimeter-wave CW source and an on-chip CMOS modulator. Off-chip millimeter-wave source module will increase the size, the total power consumption and the cost of the TX system. The oscillator should be embedded in the CMOS chip for a practical application. The millimeter-wave CMOS oscillators are commonly designed in differential

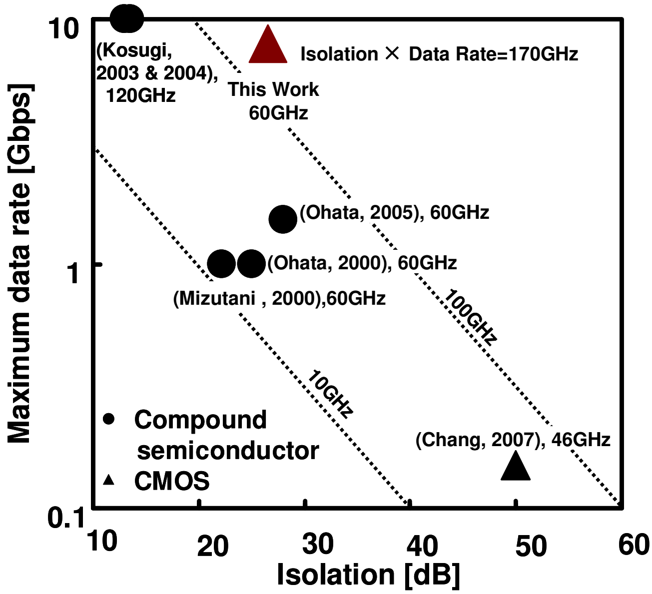

Fig. 20. Maximum data rates as a function of isolation of the ASK modulators.

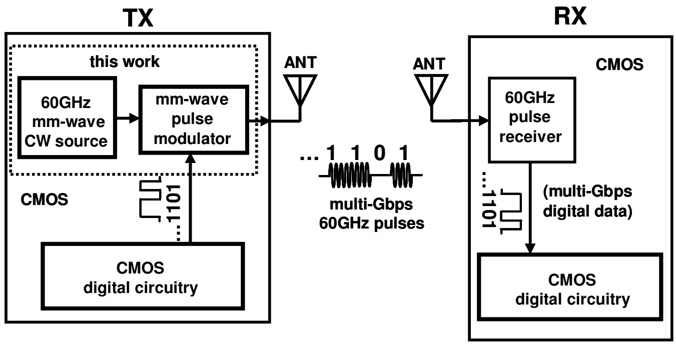

Fig. 21. Block diagram of a Giga-bit millimeter-wave wireless pulse communication in CMOS.

ended (Huang, 2006). In this design a differential ended CMOS oscillator was designed for a 60GHz CW source. To utilize the differential-ended output signal, a double-pole-single-throw (DPST) switch was proposed for modulator as shown in Fig. 22(b).

2.3.1 60GHz pulse transmitter design

2.3.1.1 60GHz CMOS CW Signal Source Design

Figure 23 shows the schematic of the on-chip 60GHz CW source circuit which consist of two sub-blocks, a 60GHz oscillator and a buffer. The oscillator generates a 60GHz CW signal and the buffer drives the ASK modulator. The 60GHz oscillator contains an on-chip transmission

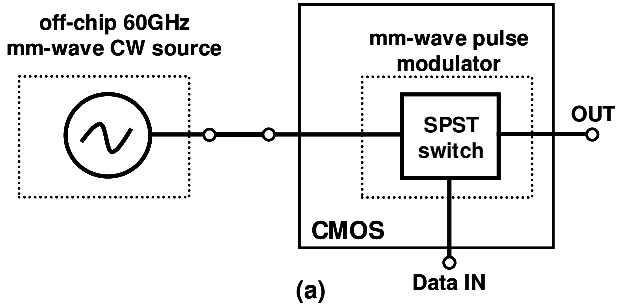

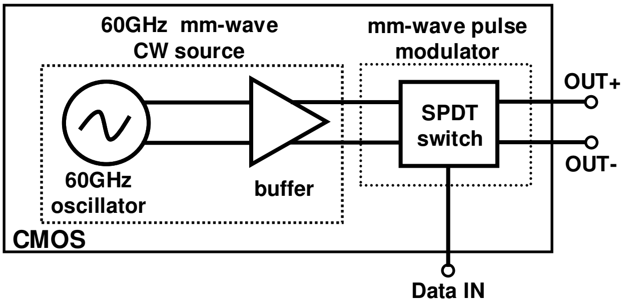

Fig. 22. Architecture of (a) a single-ended millimeter-wave pulse transmitter with off-chip 60GHz CW source and (b) a proposed differential-ended pulse transmitter with on-chip 60GHz CW source.

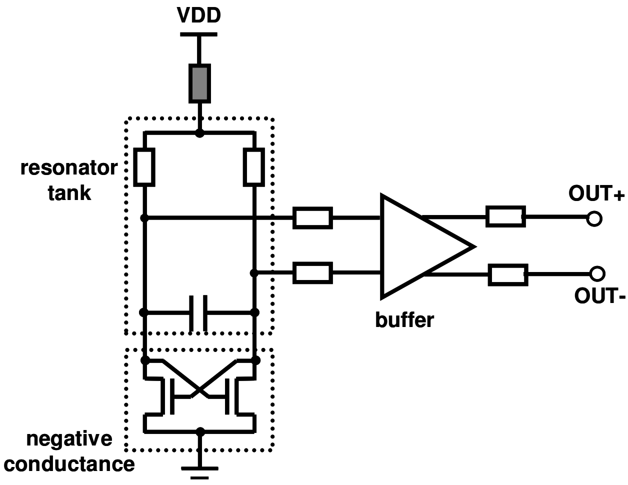

Fig. 23. Circuit schematic of a 60GHz millimeter-wave continues-wave (CW) source.

line resonating tank with a MOS capacitor and two cross-coupled MOSFETs which realize a negative conductance in parallel with the tank. The size of the devices was chosen by considering the parasitic and the process variations to keep the resonation at the 60GHz millimeter-wave band. The active device and the MOS capacitor models were obtained from the foundry. The transmission lines were characterized by a 3D full-wave electromagnetic field simulation using high-frequency structure simulator (HFSS).

The bias voltage does not only affect the negative conductance but also power consumption. High supply voltage results in a high-power dissipation. Even though a maximum 1.2V supply voltage is allowed in this CMOS process, it is simulated in spectre RF that the oscillation starts when the supply voltage is approximately 0.9V. 0.1V was decided as a margin and the supply voltage was set to be 1V for low-power operation.

2.3.1.2 Millimeter-wave Differential Ended CMOS ASK Modulator Design

Figure 24 shows the 60Hz differential ended CMOS ASK modulator. It is designed by a DPST switch consisting of a parallel connected two SPST switches. The inputs are connected to the complementary outputs of the on-chip 60GHz signal source. The gates of the switches are controlled by binary data. Each SPST switch is designed with two NMOSFET switches and a transmission line, TL1 as shown in Fig. 24. When the digital input is 0V, the NMOSFET switches are turned off. Since the parasitic capacitance of each switch in the OFF state is negligible, the input impedance of each transmission line is equal to the load impedance and the input power is transferred to the output as shown in Section 2.2 Fig. 12(a). When the digital input is 1V, the switches are turned on. The transmission line transforms the low impedance of the switch to high impedance and reflection is increased. In this case, the leaked power to the output is reduced and isolation is improved as shown in Section 2.2 Fig. 12(b).

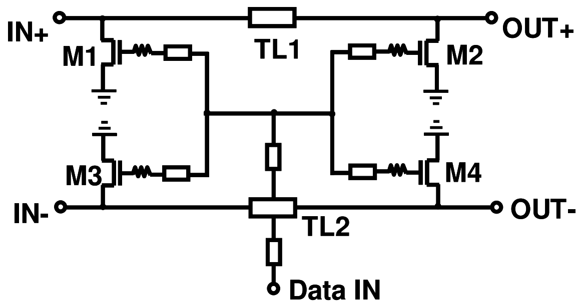

Fig. 24. Circuit schematic of the differential-ended ASK modulator for 60GHz millimeter-wave pulse transmitter.

The isolation is theoretically maximized when the switches are separated by a quarter-wavelength transmission line however long transmission lines result higher insertion loss. The isolation was maximized with two quarter-wavelength transmission lines whose total length is 900μm which results in 6.6dB insertion loss in Section 2.2. The isolation is nearly flat from 20 to 80GHz, although the maximum isolation is measured at 60GHz. As a result, shorter transmission lines may be adopted to reduce the insertion loss caused by the on-chip transmission line in the ON state of the modulator. In this CMOS technology, the length of a quarter-wavelength transmission line is 600μm. We designed the switch with a 300μm long transmission line where the isolation will slightly degrade but the insertion loss will improve.

2.3.2 60GHz pulse transmitter measurement and discussions

The proposed pulse transmitter, a 60GHz millimeter-wave source and an ASK modulator test circuits were fabricated by an 8-metal-1-poly 90nm CMOS process with a rewiring layer fabricated by a wafer-level chip-scale package (W-CSP). Figure 25 shows the micrographs of the pulse transmitter chip. In this design, the pitch of radio frequency and the biasing pads are designed 150μm.

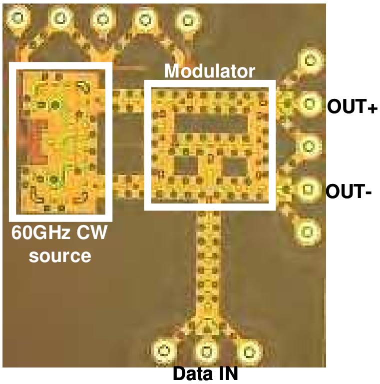

Fig. 25. Micrograph of the fabricated 60GHz pulse transmitter chip.

2.3.2.1 60GHz CW signal source

The spectrum of the 60GHz CW signal source was measured using an Agilent E4407B spectrum analyzer and an Agilent 11970V 50-75GHz harmonic mixer. A 60GHz continues-wave signal was measured at the output of the circuit whose spectrum is shown in Fig. 26. In this measurement setup, the total power loss of the probe, cables, connecters and harmonic mixer is approximately 42dB. It was observed that the fabricated chip starts to oscillate when the bias voltage is larger than 0.7V. The measured operating frequency as a function of supply voltage is plotted in Fig. 27(a). Figure 27(b) shows the power dissipation and millimeter-wave RF power as a function of the supply voltage from 0.7V to 1.4V. As the supply voltage increases, the power dissipation rapidly increases. However, the millimeter-wave output power saturates when the supply voltage reaches near to 1V. The power

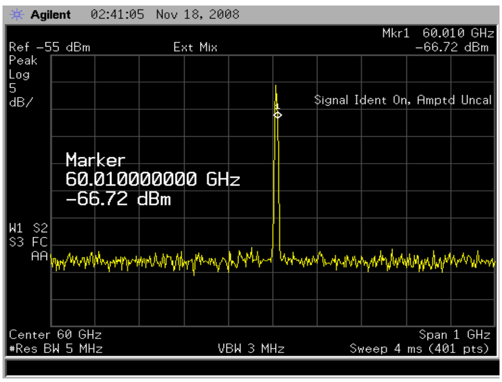

Fig. 26. Measured output spectrum of the 60GHz CW source.

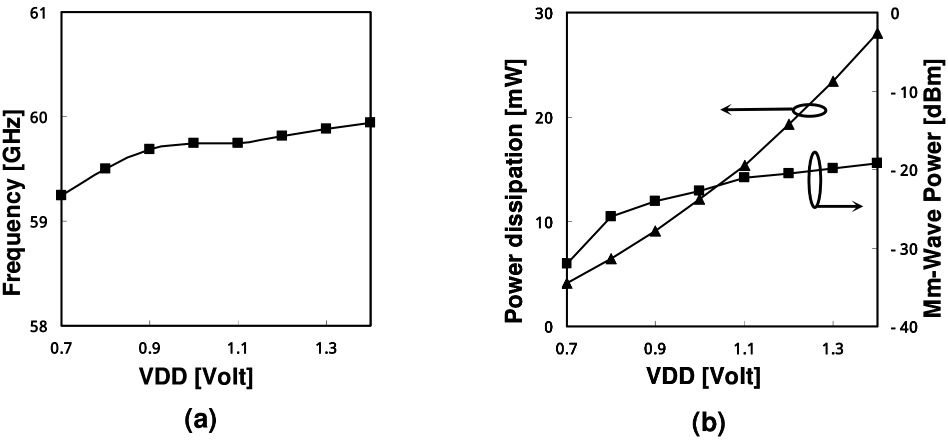

Fig. 27. Measured (a) operating frequency of the oscillator and (b) power dissipation and output millimeter-wave power of the oscillator as a function of supply voltage.

dissipation was measured to be a 19.2mW at a maximum allowed supply voltage of 1.2V. We reduced to the supply voltage to 1V for low-power operation where the millimeter-wave output power was measured to be -20.7dBm and power dissipation of 12.1mW. In this study, we found out that our layout versus schematic verification software had not been functioning properly while we had been designing the circuit using this 90nm CMOS technology first time. The core of the oscillator operates properly; however, because of the verification error in the layout, we noticed that the buffer attenuates the generated millimeter-wave signal by 18dB although it was designed to have 10dB gain.

2.3.2.2 Millimeter-wave CMOS ASK Modulator

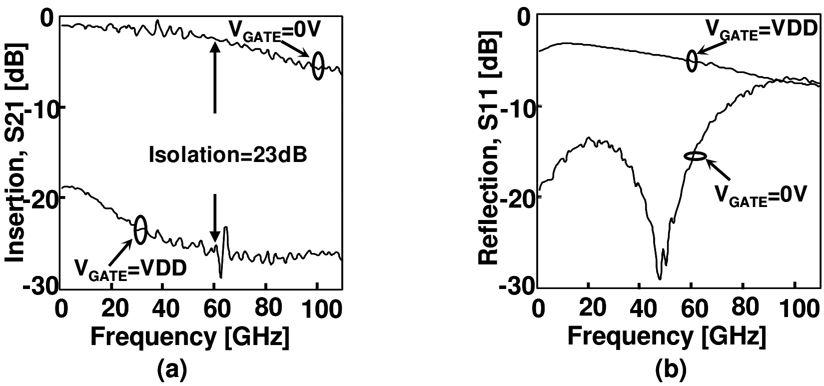

Fig. 28. Measured (a) insertion loss (S21) and (b) reflection loss (S11) of the ASK modulator for ON and OFF states.

The scattering parameters of the ASK modulator test circuit were measured on-wafer up to 110GHz with Anritsu ME7808 network analyzer with transmission reflection modules for